Design and Optimization of UAV-Aided ISAC System for Efficient Search and Rescue

Yusong Huang[1], Yongwei Zhang[1] Murat Temiz [2]
[1]School of Transportation and Civil Engineering, Nantong University, Nantong, JS 226019, China
[2]Department of Electronic and Electrical Engineering, University College London, WC1E 7JE, London, UK
*Corresponding author: Yongwei Zhang (david.y.zhang@ntu.edu.cn)
Emails: hys0028@stmail.ntu.edu.cn, david.y.zhang@ntu.edu.cn, m.temiz@ucl.ac.uk

***Abstract*—Unmanned aerial vehicles (UAVs) are increasingly playing an active role across various industry sectors. Sensing is one of the key prospects, enabling Integrated Sensing and Communication (ISAC)-aided UAVs to operate more effectively in complex situations, particularly in time-critical applications such as search and rescue. This paper proposes a unified design framework for UAV-borne ISAC systems. We first develop a comprehensive propagation model that accounts for both communication links and radar echoes. Then, to address the nonconvexity of jointly optimizing beamforming and power allocation for maximizing target detection probability under transmit power and per-user Signal-to-Interference-plus-Noise Ratio (SINR) constraints, we proposed a semidefinite relaxation (SDR)-based method to reformulate the problem into a convex approximation. Slack variables and penalty factors were introduced to achieve a flexible trade-off between sensing and communication objectives. Numerical results demonstrate that the proposed joint trajectory and beamforming optimization method enabled UAV-borne ISAC platforms to reach a moderate balance between user communication rates and Signal-to-Noise Ratio (SNR) for sensing along the predetermined searching path.**

***Index Terms*—ISAC, UAV, Search and Rescue, Beamforming, Power Allocation, SDR, Target Detection, Optimization**

I. Introduction

Integrated sensing and communication (ISAC) systems offer both sensing and communication functions using the same waveform and platforms to improve the spectral efficiency and energy efficiency [1], [2]. The integration of ISAC on unmanned aerial vehicles (UAVs) has emerged as a promising solution for time-critical missions such as search and rescue, disaster monitoring, and environmental surveillance [3]–[5]. In search and rescue operations, where rapid target localization and reliable team communication are paramount, UAV-borne ISAC platforms offer significant advantages by sharing both spectrum and hardware resources. This integration can simultaneously support high-rate data links to ground users (e.g., rescue teams) and high-resolution target detection, overcoming the spectral inefficiency and hardware redundancy of separate systems [6].

In a standard UAV-borne ISAC scenario, the aerial platform navigates a predefined trajectory while transmitting a joint waveform for downlink communication and radar sensing [7], [8]. ISAC systems can be designed based on existing communication or sensing waveforms [9], [10]. On the other hand, effective operation requires careful design of flight paths, beamforming, and power allocation to balance the trade-off between communication quality-of-service (QoS) and sensing performance [11]–[15]. Here, QoS refers to quality of service, typically measured by user-level metrics such as signal-to-interference-plus-noise ratio (SINR), while sensing performance may be evaluated in terms of signal-to-noise ratio (SNR) or target detection probability. However, the resulting joint optimization problem is often nonconvex due to the coupled nature of SINR and detection probability constraints.

While existing studies have explored UAV-ISAC extensively—addressing diverse aspects such as stringent QoS requirements, adaptable ISAC design, multi-UAV systems, and reconfigurable intelligent surfaces (RIS)-assisted implementations [16], as well as real-time trajectory optimization, joint maneuver and beamforming, target tracking [17], target localization, periodic sensing, and even integrated sensing, communication, and computing—effectively addressing this non-convexity to maximize target detection probability under stringent communication QoS in dynamic search and rescue environments, particularly through a practical and robust optimization framework, remains a key challenge.

To tackle this challenge and balance the competing demands of sensing and communication, this paper proposes a unified design framework for UAV-borne ISAC in search and rescue missions. We first develop a comprehensive propagation model that incorporates both one-way communication links and two-way radar echoes. To maximize target detection probability—a critical factor in swift rescue—under per-slot transmit power and per-user SINR requirements, we reformulate the original nonconvex problem using semidefinite relaxation (SDR), transforming it into a tractable convex form. By introducing slack variables and penalty factors, our method enables flexible trade-offs between sensing performance and communication objectives. Numerical results show that the proposed joint trajectory and beamforming solution significantly improves average user communication rates and sensing SNR compared to baseline schemes, demonstrating its potential to enhance search and rescue effectiveness.

This work was supported in part by the NSFC under Grants 62361136811, 62174091, and 62201294, and in part by TUBITAK Grant 123N800, and METU BAP Grant AGEP-301-2025-11558.

II. System Model

A. System Configuration

We consider a UAV-assisted ISAC system as shown in Fig. 1, which comprises a rotary-wing UAV equipped with a uniform linear array (ULA) of M antennas, K single-antenna ground-based user equipments (UEs), and one ground target. At the beginning of an operational cycle T, the UAV takes off from a predetermined initial position and follows a predesigned trajectory. Throughout the cycle, the UAV communicates simultaneously with the UEs and performs target sensing by transmitting probing signals and estimating the target parameters from the corresponding echo returns. At the end of the cycle T, the UAV returns to its initial location.

For convenience, we partition the total system cycle, T, into equal-length time slots. Let N denote the total number of time slots and τ denote the duration of each time slot, where $\tau = \frac{T}{N}$. The time slots are indexed by $n \in \{1, 2, \dots, N\}$. We assume that the UAV operates at a fixed altitude H and that the UAV's position remains unchanged within each time slot.

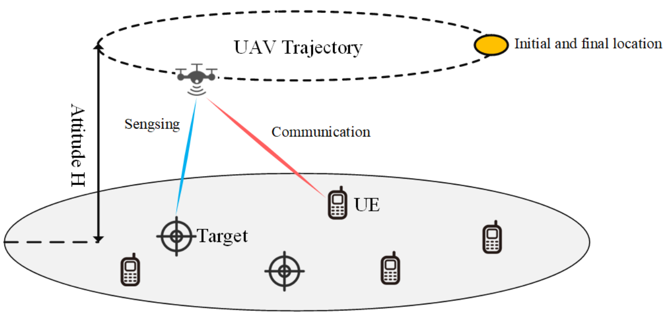

Fig. 1: The system setting.

B. Channel Model

In wireless communication systems, signals encounter complex channel environments during their propagation from the transmitter to the receiver. Taking into account both path loss and small-scale fading, we propose the following channel model to describe the channel coefficient between the m-th transmitter and the k-th receiver at time n,

$$h^c_{k,m}(n) = \frac{\rho_0}{\sqrt{H^2 + \|q(n) - q_k\|^2}} \varphi_{k,m}(n) \tag{1}$$

Let $h^c_{k,m}(n)$ denote the channel gain for the mth antenna during the nth time slot for user k. Specifically, let ρ_0 represent the channel gain when $d = 1$ and $\varphi_{k,m}(n)$ denote the communication channel gain induced by small-scale fading during the n-th time slot, which can be modeled as a complex Gaussian random variable.

For simplicity, assume that the actual propagation distance of the sensing signal is twice the distance between the UAV and the target. Let $h^s_m(n)$ denote the sensing channel gain for the m-th antenna during the n-th time slot for the target as,

$$h^s_m(n) = \frac{\beta \rho_0}{\sqrt{2\left(H^2 + \|q(n) - q_g\|^2\right)}} \varphi^s_m(n) \tag{2}$$

where, β represents the amplitude factor, and $\varphi^s_m(n)$ denotes the channel gain resulting from small-scale fading during the n-th time slot, which can be modeled as a complex Gaussian random variable.

C. Signal Model

Let the communication symbol vector at time slot n be denoted as

$$\mathbf{s}_c(n) = [s_{c,1}(n), \dots, s_{c,K}(n)]^\mathsf{T} \in \mathbb{C}^{K\times 1}, \tag{3}$$

and the sensing symbol vector as

$$\mathbf{s}_s(n) = [s_{s,1}(n), \dots, s_{s,M}(n)]^\mathsf{T} \in \mathbb{C}^{M\times 1}. \tag{4}$$

These vectors are normalized such that:

$$\mathbb{E}\left\{\mathbf{s}_c(n)\mathbf{s}_c^\mathsf{H}(n)\right\} = \mathbf{I}_K, \tag{5}$$

$$\mathbb{E}\left\{\mathbf{s}_s(n)\mathbf{s}_s^\mathsf{H}(n)\right\} = \mathbf{I}_M, \tag{6}$$

The UAV employs a ULA with M antennas. Let the communication and sensing precoding matrices at slot n be respectively$\mathbf{W}_c(n) \in \mathbb{C}^{M\times K}$ and $\mathbf{W}_s(n) \in \mathbb{C}^{M\times M}$. The integrated transmit signal is:

$$\mathbf{x}(n) = \mathbf{W}_c(n)\mathbf{s}_c(n) + \mathbf{W}_s(n)\mathbf{s}_s(n). \tag{7}$$

The transmit covariance matrix is defined as:

$$\mathbf{R}(n) = \mathbb{E}\left\{\mathbf{x}(n)\mathbf{x}^\mathsf{H}(n)\right\} = \mathbf{W}_c(n)\mathbf{W}_c^\mathsf{H}(n) + \mathbf{W}_s(n)\mathbf{W}_s^\mathsf{H}(n). \tag{8}$$

III. Problem Formulation and Transformation

A. Analysis of Data Transmission

Let $\mathbf{y}(n) \in \mathbb{C}^{K\times 1}$ denote the vector of signals received by the K users in time slot n. We can write

$$\mathbf{y}(n) = \mathbf{H}(n)\mathbf{x}(n) + \mathbf{v}(n), \tag{9}$$

where $\mathbf{H}(n) \in \mathbb{C}^{K\times M}$ is the communication channel matrix at time slot n, whose (k, m)-th element is $h^c_{k,m}(n)$, and $\mathbf{v}(n) \sim \mathcal{CN}(\mathbf{0}, \sigma^2\mathbf{I}_K)$ is the additive noise vector with independent, identically distributed complex Gaussian entries of zero mean and variance σ^2.

Let $\mathbf{h}_{c,k}(n) \in \mathbb{C}^{M\times 1}$ denote the channel vector from the UAV to user k at slot n, such that $[\mathbf{h}_{c,k}(n)]_m = h^c_{k,m}(n)$. Then the k-th component of $\mathbf{y}(n)$ is

$$y_k(n) = \mathbf{h}_{c,k}(n)^\mathsf{H}\mathbf{x}(n) + v_k(n). \tag{10}$$

Assuming the communication symbol $s_{c,k}(n)$ is intended for user k and transmitted using the k-th column of the precoding matrix $\mathbf{W}_{\rm c}(n)$, denoted by $\mathbf{w}_{{\rm c},k}(n)$, the desired received signal power for user k is

$$P_{{\rm c},k}(n) = \left|\mathbf{h}_{{\rm c},k}(n)^{\mathsf{H}}\mathbf{w}_{{\rm c},k}(n)\right|^2. \tag{11}$$

Because communication and sensing share the same spectrum, user k experiences interference from signals intended for other users (multiuser interference) and from the sensing waveform. The average multiuser interference power is

$$I_{{\rm c},k}(n) = \sum_{\substack{j=1 \\ j\neq k}}^{K}\left|\mathbf{h}_{{\rm c},k}(n)^{\mathsf{H}}\mathbf{w}_{{\rm c},j}(n)\right|^2, \tag{12}$$

and the average radar-induced interference power is

$$\begin{aligned} I_{{\rm r},k}(n) &= \mathbb{E}\left\{\left|\mathbf{h}_{{\rm c},k}(n)^{\mathsf{H}}\mathbf{W}_{\rm s}(n)\mathbf{s}_{\rm s}(n)\right|^2\right\} \\ &= \mathbf{h}_{{\rm c},k}(n)^{\mathsf{H}}\mathbf{W}_{\rm s}(n)\mathbb{E}\{\mathbf{s}_{\rm s}(n)\mathbf{s}_{\rm s}^{\mathsf{H}}(n)\}\mathbf{W}_{\rm s}(n)^{\mathsf{H}}\mathbf{h}_{{\rm c},k}(n) \\ &= \mathbf{h}_{{\rm c},k}(n)^{\mathsf{H}}\mathbf{W}_{\rm s}(n)\mathbf{W}_{\rm s}(n)^{\mathsf{H}}\mathbf{h}_{{\rm c},k}(n). \end{aligned} \tag{13}$$

Hence, the SINR for user k at slot n is

$$\mathrm{SINR}_k(n) = \frac{P_{{\rm c},k}(n)}{I_{{\rm c},k}(n) + I_{{\rm r},k}(n) + \sigma^2}. \tag{14}$$

B. Analysis of Radar Sensing

Let $P_r(n)$ denote the radar receive power at time slot n. According to the radar signal model,

$$P_r(n) = \mathbf{h}_{\rm s}(n)^{\mathsf{H}}\mathbf{R}_{\rm s}(n)\mathbf{h}_{\rm s}(n), \tag{15}$$

where $\mathbf{h}_{\rm s}(n) \in \mathbb{C}^{M\times 1}$ is the sensing channel vector at slot n, with $[\mathbf{h}_{\rm s}(n)]_m = h_m^s(n)$, and $\mathbf{R}_{\rm s}(n)$ is the covariance matrix associated with the sensing signal component of the transmission. Based on the previous definition of $\mathbf{R}(n)$, the sensing-related covariance is

$$\mathbf{R}_{\rm s}(n) = \mathbf{W}_{\rm s}(n)\mathbf{W}_{\rm s}(n)^{\mathsf{H}}. \tag{16}$$

Thus, the received radar power can be written as:

$$P_r(n) = \mathbf{h}_{\rm s}(n)^{\mathsf{H}}\mathbf{W}_{\rm s}(n)\mathbf{W}_{\rm s}(n)^{\mathsf{H}}\mathbf{h}_{\rm s}(n). \tag{17}$$

Define the target detection probability at slot n by

$$P_d(n) = Q\Big(\sqrt{2\gamma_r(n)}, \sqrt{-2\ln P_{\rm fa}}\Big), \tag{18}$$

where $Q(\cdot,\cdot)$ is the generalized Marcum Q-function (often Q_1 for first-order), $P_{\rm fa}$ is the prescribed false alarm probability, and $\gamma_r(n)$ is the received SNR for the radar return, which might be related to $P_r(n)$ normalized by noise power at the radar receiver, e.g., $\gamma_r(n) = P_r(n)/\sigma_r^2$ where σ_r^2 is the radar receiver noise variance.

C. Optimization Problem

The UAV's total transmit power for communications and sensing is subject to a maximum power constraint $P_{\max}$. To prioritize target sensing, we formulate a joint optimization over the UAV's sensing trajectory and the communication and sensing precoders. The goal is to maximize the target detection probability while guaranteeing the communication QoS for all users. Denote by $\mathbf{q}$ the UAV trajectory, and by $\{\mathbf{W}_c(n), \mathbf{W}_s(n)\}_{n=1}^N$ the sets of communication and sensing precoding matrices across N time slots. The optimization problem is stated as

$$\begin{aligned} \max_{\mathbf{W}_c(n),\,\mathbf{W}_s(n)} \quad & P_d(n) \\ \text{s.t.} \quad & \mathrm{C1}: \ \mathrm{Tr}\Big(\mathbf{W}_c(n)\mathbf{W}_c(n)^H + \mathbf{W}_s(n)\mathbf{W}_s(n)^H\Big) \\ & \qquad \le P_{\max}, \quad \forall n \in \mathcal{N}_s, \\ & \mathrm{C2}: \ \mathbf{h}_s(n)^H\,\mathbf{W}_s(n)\mathbf{W}_s(n)^H\,\mathbf{h}_s(n) \\ & \qquad \ge S_{\min}, \quad \forall n \in \mathcal{N}_s, \\ & \mathrm{C3}: \ \min_{1\le k\le K} \mathrm{SINR}_k(n) \\ & \qquad \ge \gamma_{\rm th}, \quad \forall n. \end{aligned} \tag{19}$$

where $P_d(\cdot)$ denotes the target detection probability, which is a function of the sensing trajectory and the sensing precoders. Furthermore, $\mathbf{h}_s(n)$ represents the sensing channel vector at slot n, determined by the UAV's position on its trajectory. The term $\mathrm{SINR}_k(n)$ signifies the SINR experienced by user k during slot n. Finally, $\mathcal{N}_s \subseteq \{1,\ldots,N\}$ is the set of indices for the time slots during which sensing operations are performed.

Constraint C1 ensures that the total transmit power of the UAV in each sensing time slot $n \in \mathcal{N}_s$ does not exceed the maximum allowable power $P_{\max}$, which reflects the energy budget and hardware limitations. Constraint C2 guarantees that the sensing power projected onto the direction of the target is no less than $S_{\min}$, thus ensuring reliable target detection. Constraint C3 enforces that the SINR of each user is not lower than a predefined threshold $\gamma_{\rm th}$ for all n, thereby maintaining the required communication quality.

D. Benchmark for Precoding

To contextualize the performance of the joint optimization algorithm proposed subsequently, we first establish a benchmark precoding scheme. This scheme is selected for its simplicity and low computational complexity, serving as a practical baseline for comparison. It relies on a fixed power allocation and a non-adaptive beamforming strategy, where the total transmit power $P_{\max}$ is split equally between communication and sensing tasks ($P_{\rm c} = P_{\rm s} = P_{\max}/2$).

a) Communication Precoding $\mathbf{W}_{\rm c}$*:* For the communication link, we adopt the well-known Maximum Ratio Transmission (MRT) strategy. This approach creates constructive interference at the intended receiver by aligning the transmitted signal's phase with the user's conjugate channel vector. While this maximizes the desired signal power for each user, it does not actively mitigate the resulting inter-user interference. The precoding vector for user k at time slot n, $\mathbf{w}_{{\rm c},k}(n)$, is thus defined as

$$\mathbf{w}_{{\rm c},k}(n) = \sqrt{\frac{P_{\rm c}}{K}} \cdot \frac{\mathbf{h}_{{\rm c},k}^{\mathsf{H}}(n)}{\|\mathbf{h}_{{\rm c},k}(n)\|}, \tag{20}$$

The complete communication precoding matrix $\mathbf{W}_{\rm c}(n) \in \mathbb{C}^{M\times K}$ is then formed by concatenating all precoding vectors column-wise,

$$\mathbf{W}_{\rm c}(n) = [\mathbf{w}_{{\rm c},1}(n),\, \mathbf{w}_{{\rm c},2}(n),\, \ldots,\, \mathbf{w}_{{\rm c},K}(n)]\,. \tag{21}$$

b) Sensing Precoding $\mathbf{W}_{\rm s}$*:* For the sensing link, a similar matched-filter approach is utilized. Given the single-target scenario, this simplifies to employing a single beam steered precisely towards the target's channel direction. This method ensures that the allocated sensing power is concentrated along the target's propagation path to maximize the potential strength of the radar echo. The resulting sensing precoding vector at time slot n is

$$\mathbf{W}_{\rm s}(n) = \sqrt{P_{\rm s}} \cdot \frac{\mathbf{h}_{\rm s}^{\sf H}(n)}{\|\mathbf{h}_{\rm s}(n)\|}. \tag{22}$$

The performance metrics derived from this benchmark will serve as the reference against which our proposed optimization algorithm is evaluated. It is crucial to recognize that this benchmark scheme is inherently suboptimal, as it allocates resources independently and does not actively manage the cross-interference between communication and sensing signals. To overcome these limitations and unlock the full potential of the ISAC system, we now turn to the problem of jointly optimizing the beamformers for a superior performance trade-off.

E. Joint Optimization of Communication and Sensing

The original problem of jointly optimizing communication and sensing performance—specifically, maximizing the target detection probability while guaranteeing minimum communication rates—constitutes a non-convex optimization problem. The sources of nonconvexity primarily stems from the bilinear terms in the signal power expressions and the fractional form of the SINR constraints when directly optimizing the precoding matrices.

To address this issue, we reformulate the problem using SDR. Specifically, we lift the beamforming vectors $\mathbf{w}_{{\rm c},k}(n)$ and $\mathbf{W}_{\rm s}(n)$ into higher-dimensional Hermitian PSD transmit covariance matrices and remove the non-convex rank-one constraints. This transforms the original problem into a convex SDP, which retains the structure of the power and interference constraints while enabling tractable optimization via standard convex solvers.

Since the target detection probability $P_d(n)$ increases monotonically with the received radar signal power $P_r(n)$, or equivalently, the sensing SNR χ, maximizing $P_d(n)$ is equivalent to maximizing χ. Therefore, for the single-target case, we adopt the strategy of maximizing χ under communication QoS constraints.

The optimization variables include the communication covariance matrices $\mathbf{R}{\rm c}, k(n) \in \mathbb{C}^{M\times M}$ for each user k and the sensing covariance matrix $\mathbf{R}{\rm s}(n) \in \mathbb{C}^{M\times M}$. The objective is to maximize the sensing SNR χ, while non-negative slack variables δ_k are introduced to relax the SINR constraints and enable trade-offs between communication and sensing performance. These slack variables are penalized in the objective via a weighting factor λ.

As a result, the problem for each time slot n is reformulated as a convex SDP that jointly optimizes $\mathbf{R}{\rm c}, k(n)$ and $\mathbf{R}{\rm s}(n)$ to balance sensing SNR maximization and communication QoS guarantees. The joint communication and sensing optimization problem is reorganized as an SDP, subject to several practical constraints:

$$\max_{\substack{\mathbf{R}_{{\rm c},k}(n),\mathbf{R}_{\rm s}(n),\\ \chi,\{\delta_k\}}} \quad \chi - \lambda \sum_{k=1}^{K} \delta_k \tag{23a}$$

$$\text{s.t.} \quad \mathbf{h}_{\rm s}(n)^{\sf H}\mathbf{R}_{\rm s}(n)\mathbf{h}_{\rm s}(n) \geq \chi, \tag{23b}$$

$$\mathbf{h}_{{\rm c},k}(n)^{\sf H}\mathbf{R}_{{\rm c},k}(n)\mathbf{h}_{{\rm c},k}(n) + \delta_k \geq \gamma_{\rm th}\Big(\sum_{j\neq k}\mathbf{h}_{{\rm c},k}(n)^{\sf H}\mathbf{R}_{{\rm c},j}(n)\mathbf{h}_{{\rm c},k}(n) + \mathbf{h}_{{\rm c},k}(n)^{\sf H}\mathbf{R}_{\rm s}(n)\mathbf{h}_{{\rm c},k}(n) + \sigma^2\Big), \quad \forall k \tag{23c}$$

$$\sum_{k=1}^{K} {\rm Tr}\left(\mathbf{R}_{{\rm c},k}(n)\right) + {\rm Tr}\left(\mathbf{R}_{\rm s}(n)\right) \leq P_{\max}, \tag{23d}$$

$$\sum_{k=1}^{K} {\rm Tr}\left(\mathbf{R}_{{\rm c},k}(n)\right) \geq P_{\min}, \tag{23e}$$

$$\mathbf{R}_{{\rm c},k}(n) \succeq \mathbf{0}, \quad \mathbf{R}_{\rm s}(n) \succeq \mathbf{0}, \quad \forall k, \tag{23f}$$

$$\chi \geq S_{\min}, \quad \delta_k \geq 0, \quad \forall k. \tag{23g}$$

- **Sensing SNR Constraint (Eq.** (23b) **& Eq.** (23g)**):** The radar sensing SNR must exceed $S_{\min}$ to guarantee reliable target detection performance. This is jointly captured by the auxiliary sensing performance variable χ and its lower bound $S_{\min}$.
- **Communication SINR Constraint (Eq.** (23c)**):** Each communication user must receive a signal with SINR no less than $\gamma_{\rm th}$ to meet QoS requirements. This includes multi-user interference, sensing interference, and noise.
- **Minimum Communication Power Constraint (Eq.** (23e)**):** The sum power allocated to all communication users must be greater than $P_{\min}$ to ensure a baseline level of service.
- **Total Transmit Power Constraint (Eq.** (23d)**):** The UAV's total transmit power must not exceed $P_{\max}$, reflecting hardware limitations and energy efficiency considerations.
- **Semidefinite and Non-negativity Constraints (Eq.** (23f) **& Eq.** (23g)**):** All transmit covariance matrices must be Hermitian positive semidefinite, and auxiliary variables like δ_k and χ must be non-negative.

In the formulation, σ^2 and σ_r^2 denote the noise variances at the communication users and radar receiver, respectively. The matrix constraint $\mathbf{A} \succeq \mathbf{0}$ indicates that $\mathbf{A}$ is Hermitian positive semidefinite. The optimal solutions are given in terms of the transmit covariance matrices $\mathbf{R}_{{\rm c},k}^*(n)$ for communication and $\mathbf{R}_{\rm s}^*(n)$ for sensing. Since the obtained $\mathbf{R}_{{\rm c},k}^*(n)$ may not be rank-1, which is required for practical beamforming implementation, a post-processing step is applied. Specifically, a rank-1 approximation is performed by extracting the principal eigenvector corresponding to the largest eigenvalue, yielding the final beamforming vectors $\mathbf{W}_{c,k}(n)$.

IV. Numerical Results

A. System Parameters

The key system simulation parameters used in our evaluations are summarized in Table I.

TABLE I: The key parameters of system simulation.

Parameter (Unit)	**Symbol**	**Value**
UAV flight altitude (m)	H	50
Circular trajectory radius (m)	–	300
Number of UAV antennas	M	4
Number of communication users	K	3
Reference channel gain	ρ_0	1×10^{-2}
Communication noise variance (W)	σ^2	1×10^{-10}
Sensing noise variance (W)	σ_r^2	1×10^{-10}
Total transmit power (W)	P_{max}	20
Communication SINR threshold	γ_{th}	1
Penalty factor for slack variables	λ	1×10^6
Minimum user power (W)	$P_{\text{min\_user}}$	1

B. Simulation Results

Fig. 2 shows the average sensing SNR over 100 time slots. While there are fluctuations where the baseline performs comparably, the proposed joint precoding method generally yields a higher sensing SNR, particularly in achieving higher peak values. As stated in the original study, on average, a 2 dB improvement is observed, which confirms the overall effectiveness of our optimization in enhancing the system's sensing capabilities.

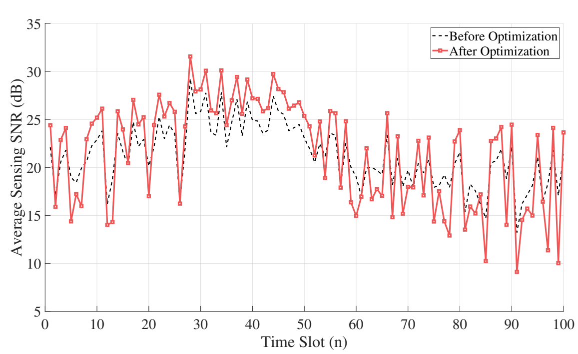

Fig. 2: Average sensing SNR over time: proposed joint optimization vs. baseline scheme.

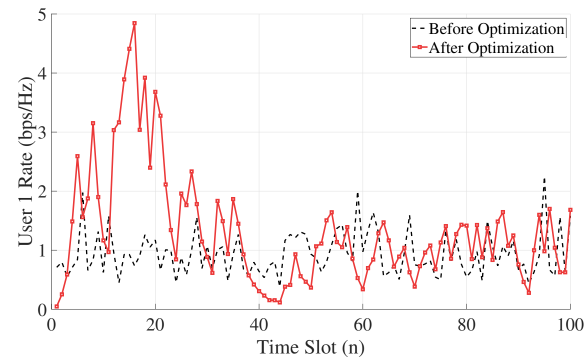

(a) User 1

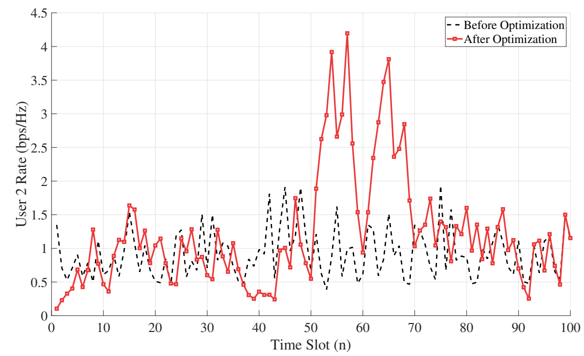

(b) User 2

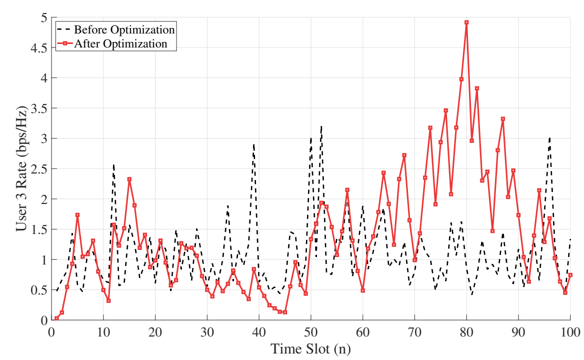

(c) User 3

Fig. 3: Instantaneous communication rates over time along the trajectory, the performance of communication is compared between the joint optimization and direct calculation.

Fig. 3 provides a detailed view of the instantaneous communication rates, illustrating a clear correlation between the UAV's position on its circular trajectory and each user's performance. The proposed method (solid red line) enables significantly higher peak data rates compared to the baseline (dashed black line).

- **For User 1 (Fig. 3a):** The data rate reaches its maximum during the first quarter length of the total trajectory for simulation, specifically within the 10 to 25 time-slot window. A sharp peak of nearly 5 bps/Hz is visible around time slot 18. This strongly suggests that the UAV is flying closest to User 1 during this period, resulting in the most favorable channel conditions.
- **For User 2 (Fig. 3b):** The period of highest performance for User 2 occurs much later. The data rate reach the peak in the 55 to 70 time-slot window, obtaining the data rate over 4 bps/Hz around time slot 55. This reflected the fact that the UAV is close to User 2 during the second half of its trajectory.

- **For User 3 (Fig. 3c):** User 3 experiences the best channel conditions towards the end of the travel time. Its data rate is significantly high in the 75 to 90 time-slot window, with a peak over 4 bps/Hz occurring around the time slot 80.

At the time slot 10, communication rates are low for the 3 communication users. At this specific moment or the time around it, the rates are low as the UAV is away from the 3 users physically, and close to the target for sensing, hence the probability of detection is high at this moment as depicted in Fig. 2. Another possible reason for it is that the interference from the target reflection is strong at this moment.

It is noted at the time slot 60, the data rate for user 2 is low even though physically the UAV is approximately above User 2 at that time, the reason is that the UAV is close to User 2, but at the same time it is also between user 1 and user 3, therefore interuser interference is high and dominated the communication performance. This is the case for User 1 and User 3, their communication performance is poor at the same time. It demonstrated the dynamic shift of propagation channel condition exerted a stringent requirement on optimization process.

V. Conclusion

This paper proposed a unified UAV-borne ISAC framework for search and rescue missions, integrating joint trajectory design, communication beamforming, and sensing covariance optimization. By leveraging SDR-based reformulation and slack variable penalization, the proposed method effectively transformed the inherent nonconvexity of the joint optimization problem into SDP.

Simulation results demonstrated that the proposed scheme leads to a notable enhancement in both sensing and communication performance. In particular, it achieves an average sensing SNR improvement of approximately 2–3 dB (roughly 30%), while also enabling significantly higher peak user data rates. These results highlighted the framework's ability to dynamically balance critical sensing and communication demands through intelligent resource allocation and mobility control over UAVs.

Future work may explore several promising directions. One natural extension is the incorporation of multi-target sensing and clutter modeling to enhance robustness in complex environments. Real-time trajectory reconfiguration, possibly assisted by reinforcement learning or predictive control, could enable adaptive responses to fast-changing mission requirements. Moreover, integrating RIS into the framework may further augment both sensing coverage and communication capacity through passive environment shaping. Finally, extending the framework to account for practical system impairments—such as channel estimation errors, hardware limitations, and energy constraints—will be essential for real-world deployment for efficient search and rescue.

References

[1] X. Fang, W. Feng, Y. Chen, N. Ge, and Y. Zhang, "Joint communication and sensing toward 6G: Models and potential of using MIMO," *IEEE Internet of Things Journal*, vol. 10, no. 5, pp. 4093–4116, 2023.

[2] M. Temiz, E. Alsusa, and M. W. Baidas, "Optimized precoders for massive MIMO OFDM dual radar-communication systems," *IEEE Trans. Commun.*, vol. 69, no. 7, pp. 4781–4794, 2021.

[3] L. Sultan, M. Anjum, M. Rehman, S. Murawwat, and H. Kosar, "Communication among heterogeneous unmanned aerial vehicles (UAVs): Classification, trends, and analysis," *IEEE Access*, vol. 9, pp. 118815–118836, 2021.

[4] A. Khan, S. Gupta, and S. K. Gupta, "Cooperative control between multi-UAVs for maximum coverage in disaster management: Review and proposed model," in *2022 2nd International Conference on Computing and Information Technology (ICCIT)*, pp. 271–277, 2022.

[5] Q. Wu, J. Xu, Y. Zeng, D. W. K. Ng, N. Al-Dhahir, R. Schober, and A. L. Swindlehurst, "A comprehensive overview on 5G-and-beyond networks with UAVs: From communications to sensing and intelligence," *IEEE Journal on Selected Areas in Communications*, vol. 39, no. 10, pp. 2912–2945, 2021.

[6] Z. Lyu, G. Zhu, and J. Xu, "Joint maneuver and beamforming design for UAV-enabled integrated sensing and communication," *IEEE Transactions on Wireless Communications*, vol. 22, no. 4, pp. 2424–2440, 2023.

[7] J. Wu, W. Yuan, and L. Hanzo, "When UAVs meet ISAC: Real-time trajectory design for secure communications," *IEEE Transactions on Vehicular Technology*, vol. 72, no. 12, pp. 16766–16771, 2023.

[8] X. Jing, F. Liu, C. Masouros, and Y. Zeng, "Isac from the sky: UAV trajectory design for joint communication and target localization," *IEEE Transactions on Wireless Communications*, vol. 23, no. 10, pp. 12857–12872, 2024.

[9] M. Temiz, E. Alsusa, and M. W. Baidas, "A dual-function massive MIMO uplink OFDM communication and radar architecture," *IEEE Transactions on Cognitive Communications and Networking*, vol. 8, no. 2, pp. 750–762, 2021.

[10] M. Temiz, C. Horne, N. J. Peters, M. A. Ritchie, and C. Masouros, "An experimental study of radar-centric transmission for integrated sensing and communications," *IEEE Transactions on Microwave Theory and Techniques*, vol. 71, no. 7, pp. 3203–3216, 2023.

[11] C. Deng, X. Fang, and X. Wang, "Beamforming design and trajectory optimization for UAV-empowered adaptable integrated sensing and communication," *IEEE Transactions on Wireless Communications*, vol. 22, no. 11, pp. 8512–8526, 2023.

[12] R. Zhang, Y. Zhang, R. Tang, H. Zhao, Q. Xiao, and C. Wang, "A joint UAV trajectory, user association, and beamforming design strategy for multi-UAV-assisted ISAC systems," *IEEE Internet of Things Journal*, vol. 11, no. 18, pp. 29360–29374, 2024.

[13] X. Liu, Y. Liu, Z. Liu, and T. S. Durrani, "Fair integrated sensing and communication for multi-UAV-enabled internet of things: Joint 3-D trajectory and resource optimization," *IEEE Internet of Things Journal*, vol. 11, no. 18, pp. 29546–29556, 2024.

[14] K. Meng, Q. Wu, S. Ma, W. Chen, K. Wang, and J. Li, "Throughput maximization for UAV-enabled integrated periodic sensing and communication," *IEEE Transactions on Wireless Communications*, vol. 22, no. 1, pp. 671–687, 2023.

[15] J. Wang, X. Zhang, F. Sun, and Z. Wei, "Joint trajectory and transmit beamforming design for UAV-enable integrated sensing, communication and computing," in *2024 16th International Conference on Wireless Communications and Signal Processing (WCSP)*, pp. 906–911, 2024.

[16] Z. Wu, X. Li, Y. Cai, and W. Yuan, "Joint trajectory and resource allocation design for RIS-assisted UAV-enabled ISAC systems," *IEEE Wireless Communications Letters*, vol. 13, no. 5, pp. 1384–1388, 2024.

[17] Y. Jiang, Q. Wu, W. Chen, and K. Meng, "UAV-enabled integrated sensing and communication: Tracking design and optimization," *IEEE Communications Letters*, vol. 28, no. 5, pp. 1024–1028, 2024.